The Hercules-Aquila Cloud and Virgo Overdensity with Gaia DR2

Keith T. Smith,[1]⋆ A. N. Other,[2] Third Author[2,3] and Fourth Author[3]

[1]*Royal Astronomical Society, Burlington House, Piccadilly, London W1J 0BQ, UK*
[2]*Department, Institution, Street Address, City Postal Code, Country*
[3]*Another Department, Different Institution, Street Address, City Postal Code, Country*

ABSTRACT

200 words for Letters. No references should appear in the abstract.

Key words: keyword1 – keyword2 – keyword3

1 INTRODUCTION

Introduction.

2 DATA AND ANALYSIS

Two samples of RR Lyrae with line-of-sight velocity measurements have been combined in this work to study the HAC and the VOD. Vivas et al. (2016) compiled a catalog of 412 RRL in the region of the VOD with distances between 4 and 75 kpc from the Sun. Simion et al. (2018) provides the radial velocities for 46 HAC RRL in a narrow distance range, between 15 and 18 kpc, where the peak of the HAC overdensity lies Simion et al. (2014).

2.1 6-D Phase space measurements

44 of the 46 stars in table 1 in Simion et al. (2018) and 411 of the 412 in table 4 in Vivas et al. (2016) with matches within 2" in the Gaia DR2 catalog, have proper motion measurements.
The only star in the VOD region without proper motion measurement, belongs to a 'high-significance' kinematical group (group 1), likely the Sagittarius stream, identified by Vivas et al. (2016). 113 stars (112 with proper motions) belong to this group and we have excluded them for the analysis as a major contaminant of the VOD field. The spatial distribution of the remaining stars (44 from Simion et al. 2018 and 299 from Vivas et al. 2016) with full 6-D phase space measurements is illustrated in Figure 1, in Galactic coordinates (left panel) and in the Galactic plane and perpendicular to the Galactic plane projections. We adopted left-handed Galactic Cartesian coordinates with the Sun located at $(x_\odot, y_\odot, z_\odot) = (-8, 0, 0)$ kpc, the X-axis positive in the direction of the Galactic center, Y-axis oriented along the Galactic rotation and the Z-axis directed towards the north Galactic pole.
Vivas et al. 2016 identified 6 significant kinematical groups in the VOD field (their table 5) but only groups 1 and 2 (likely members of the VOD, with $< v_{GSR} >= 135$ km/s) contain more than 10 stars. We mark group 2 with green circles.

2.2 Velocity distribution

The velocity distribution in spherical polar coordinates (v_r, v_θ, v_ϕ are the radial, azimuthal and polar components respectively) are shown in Fig. 2. To estimate the error on each velocity component we resample the data 1000 times from a multivariate Gaussian distribution with mean the measurement $\{ra^i, dec^i, d^i, pmra^i, pmdec^i, v_h^i\}$ and full covariance matrix which takes into account the covariances between ra, dec and proper motions, provided by Gaia DR2. We take the standard deviation of the resulting $\{v_r, v_\theta, v_\phi\}$ distributions as the upper limit of the velocity uncertainties. These errors are reported for all stars in Fig. 2. *Here I need to comment on the error bars, why so big for VOD, eg. higher distance, pm error etc.*
The orbital anisotropy, is highly radial in the HAC field ($\beta = 0.91 \pm 0.03$) where the stars are most likely members of the Cloud and radial in the VOD field ($\beta = 0.74 \pm 0.04$) in which stars span a much wider range of distances. The anisotropy values are the median and standard deviation over 500 non parametric bootstrap resampling trials.
Fig. 3 shows the behaviour of the VOD azimuthal v_θ and radial v_r distributions in 3 distance slices above the Galactic plane. In each slice we have calculated the fraction of Oosterhoff type I (Oo I) RR Lyrae, using equations 1 and 2 in Belokurov et al. (2018) to classify the RRL into two types. According to this classification, Oosterhoff type II (Oo II) RR Lyrae will incude both Oo II and Intermediate objects. In the 10<z/kpc<20 range, where the orbital anisotropy is the highest ($\beta = 0.84 \pm 0.03$), the Oo I type dominates (77%),


⋆ E-mail: mn@ras.org.uk (KTS)
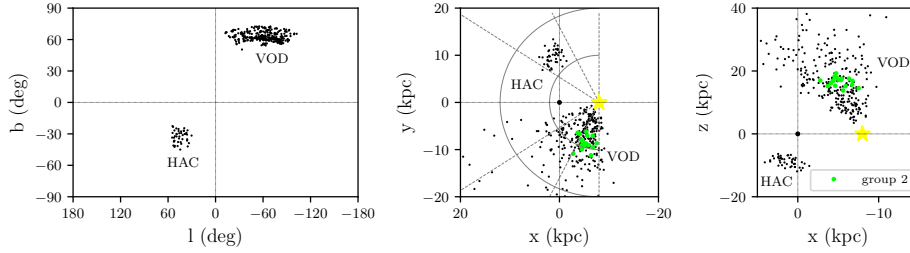
Figure 1. Spatial distribution of the RR Lyrae used in this work with full 6-D phase space measurements, in Galactic coordinates (left panel) and in the $x - y$ (middle) and $y - z$ (right) planes. The HAC field contains 44 RR Lyrae which likely belong to the Cloud with measured line-of-sight velocities (Simion et al. 2018) and Gaia DR2 proper motions. The VOD field contains 411 RRL which belong to several halo associations, including the Sagittarius stream and the VOD, with line-of-sight velocities provided by Vivas et al. 2016 and proper motions from Gaia DR2. In particular we mark group 2, a 'high significance' kinematical group, which contains 18 stars (green circles). The semi-circles are centred on the Sun's position and have radius of 10 and 20 kpc. The Sun (yellow star) is located at $(x_\odot, y_\odot, z_\odot) = (0,-8,0)$ kpc and the Galactic centre at $(0,0,0)$ - black circle.
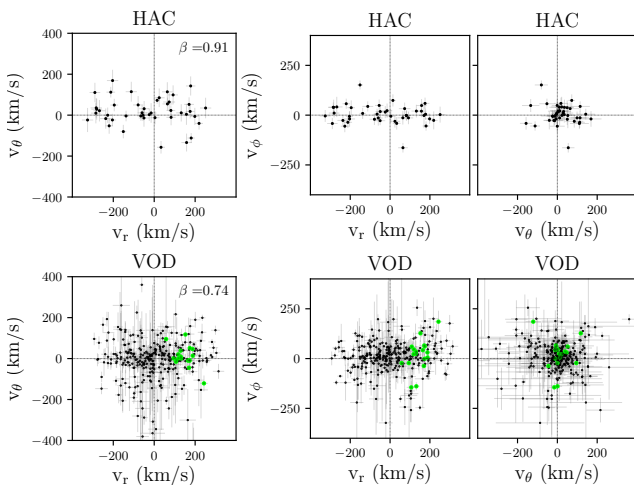
Figure 2. RRL velocity distribution in spherical polar coordinates (v_r, v_θ, v_ϕ are the radial, azimuthal and polar components respectively) in the HAC field (top row) and the VOD field (middle and bottom rows). The error on the velocity components of each star i, $[\sigma_{v_r}^i, \sigma_{v_\theta}^i, \sigma_{v_\phi}^i]$, has been propagated by randomly drawing 1000 stars from a multivariate Gaussian distribution with mean the measurement $(ra^i, dec^i, d^i, pmra^i, pmdec^i, v_h^i)$ and full covariance matrix (takes into account the covariances between ra,dec and proper motions). The orbital anisotropy, is highly radial in the HAC field ($\beta = 0.91 \pm 0.03$) where the stars are most likely members of the Cloud and mildly radial in the VOD field ($\beta = 0.74 \pm 0.04$) in which stars span a much wider range of distances (see Fig. 1).
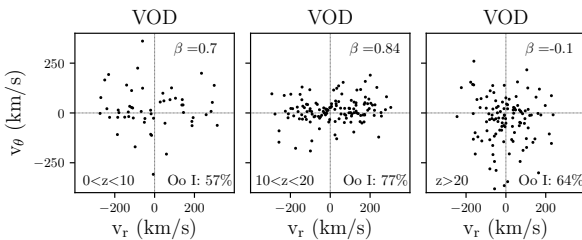
Figure 3. Radial versus azimuthal velocity in the VOD field, in three distance ranges above the Galactic plane. The fraction of RR Lyrae of Oosterhoff type I is reported in each panel.
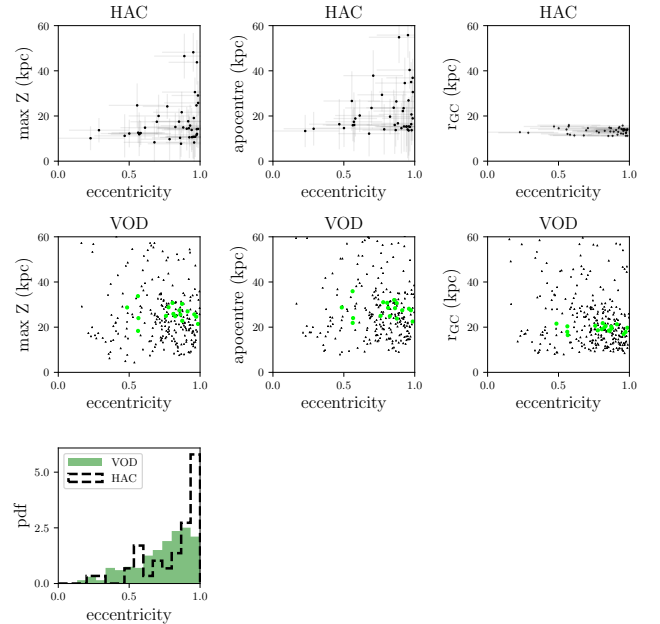

Figure 4. Orbital properties of the stars in the HAC and VOD fields. 'group 2' has similar orbital properties to the HAC, however it does not display a sausage velocity distribution (see middle row figure 2) - they are concentrated at $vr = 135$km/s as calculated by Vivas et al. 2016.

as in the HAC field (note: add number here). In the same slice, 73% of the stars belong to the 'sausage' component. The same behaviour but less accentuated can be noticed in the 0<z/kpc<10 slice where $\beta = 0.7 \pm 0.1$ is less radial but the fraction of Oo I stars decreases drammatically (note: comment if this is expected?). Further from the plane, at z>20 kpc, the velocity ellipsoid is almost isotropic with $\beta = -0.1 \pm 0.2$. We have excluded the most likely members of the Sagittarius stream but several others may remain, decreasing β.

2.3   Orbital properties of the HAC and VOD

We integrate orbits using the **galpy** package Bovy (2015) in the recommended MWPotential2014 model for the Galactic
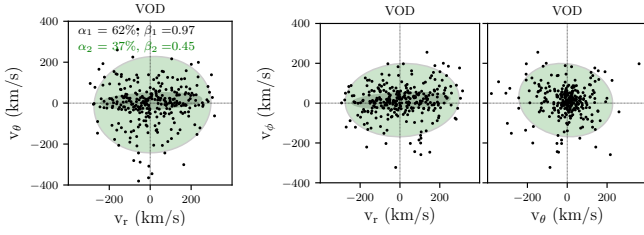
Figure 5. Result of the extreme deconvolution.
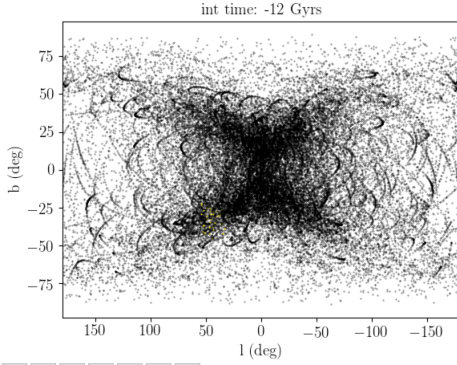
Figure 6. The backward orbit integration for HAC only. Plot needs updates. Also, issue with doubling the mass of the MW in galpy, normalisation should be 0.35 for the NFW potential (concentration?).

potential which is composed of a Miyamoto-Nagai disc, a bulge with a power-law density profile that is exponentially cut-off, and a dark matter halo described by a NFW potential. The parameters are given in table 1 Bovy (2015). The resulting orbital properties are given in Fig 4. To compute the errors (not shown for VOD to simply the figure) we integrated 500 orbits for each star where the orbits were initialised on parameters resampled from data, as in the previous section. The pdf of the eccentricities is also shown.

3 DISCUSSION

3.1 ED of the VOD field

Figure 5 goes here.

3.2 Are the VOD and HAC related?

Backward orbit integration. It will be Figure 6.

4 CONCLUSIONS

REFERENCES

Belokurov V., Deason A. J., Koposov S. E., Catelan M., Erkal D., Drake A. J., Evans N. W., 2018, MNRAS, 477, 1472
Bovy J., 2015, ApJS, 216, 29
Simion I. T., Belokurov V., Irwin M., Koposov S. E., 2014, MNRAS, 440, 161
Simion I. T., Belokurov V., Koposov S. E., Sheffield A., Johnston K. V., 2018, MNRAS, 476, 3913
Vivas A. K., Zinn R., Farmer J., Duffau S., Ping Y., 2016, ApJ, 831, 165

This paper has been typeset from a TeX/LaTeX file prepared by the author.